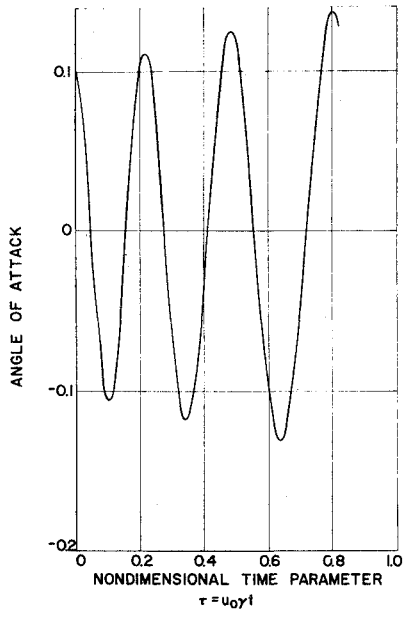

Fig. 1 Motion for P = 1000, and zero aerodynamic damping. a_0 = 0.1 rads.

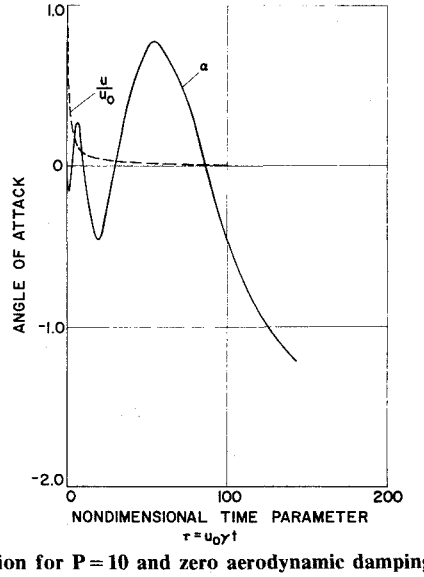

Fig. 2 Motion for P = 10 and zero aerodynamic damping. a_0 = 0.1 rads.

The motion will diverge or converge, depending on whether m is positive or negative. Note that

$$e^{m\eta} = e^{m\log(1+\tau)} = (1+\tau)^m = (1+\tau)^{(\frac{1}{2}+\psi_1/2\gamma)} \tag{10}$$

Thus the criteria for reducing amplitude is

$$1+(\psi_1/\gamma)<0$$

or

$$(C_{m_{\dot\alpha}}/C_D) < -(r_G/\ell)^2 \tag{11}$$

where r_G is the radius of gyration ($I = mr_G^2$), and ℓ is the characteristic length on which the moment coefficients are based.

Suppose the speed drops to $u^* = zu_0 (z<1)$. From Eq. (2), the associated time parameter is given by

$$z = 1/(1+\tau^*)$$

Thus from Eq. (1), the ratio

$$\frac{\alpha^*_{\max}}{\alpha_0} = z^{-\frac{1}{2}\left[1+(C_{m_{\dot\alpha}}/C_D)(\ell/r_G)^2\right]} \tag{12}$$

For example, if $C_{m_{\dot\alpha}} = 0$, then at half the initial speed ($z = 0.5$),

$$\alpha^*_{\max} = \sqrt{2}\,\alpha_0$$

This result is independent of the number of oscillatory cycles involved. That is, it is independent of the "aerodynamic stiffness."

The oscillatory frequency is

$$\Omega = \frac{d\theta}{dt} = \frac{d}{d\eta}(n\eta)\frac{d\eta}{d\tau}\frac{d\tau}{dt} = \frac{nu_0\gamma}{1+\tau}$$

$$= (\tfrac{1}{2}u_0\sqrt{-[(\gamma+\psi_1)^2+\psi_2]}/(1+u_0\gamma t) \tag{13}$$

so that instantaneous frequency is diminishing with time. If $C_{m_{\dot\alpha}} = 0$, the motion depends uniquely on τ and the dimensionless parameter

$$P = \frac{\psi_2}{\gamma^2} = \frac{C_{m_\alpha}}{C_D^2}\cdot\frac{2\ell m}{\rho S r_G^2} \tag{14}$$

Solutions for $P = 1000$ and 10 are plotted in Figs. 1 and 2.

References

[1] Friedrich, H.R. and Dore, F.J., "The Dynamic Motion of a Missile Descending Through the Atmosphere," *Journal of Aeronautical Sciences*, Sept. 1955, pp. 628-638.

[2] Allen, H.J., "Motion of a Ballistic Missile Angularly Misaligned with the Flight Path Upon Entering the Atmosphere and its Effect upon Aerodynamic Heating, Aerodynamic Loads, and Miss Distance," NACA TN 4048, Oct. 1957.

[3] Allen, H.J. and Eggers, A.J., Jr., "A Study of the Motion and Aerodynamic Heating of Ballistic Missiles Entering the Earth's Atmosphere at High Supersonic Speeds," NACA Rept. 1381, 1958.

[4] Tobak, J. and Allen, H.J., "Dynamic Stability of Vehicles Traversing Ascending or Descending Paths Through the Atmosphere," NACA TN 4275, July 1958.

[5] Laitone, E.V., "Dynamic Longitudinal Stability Equations for Re-Entry Ballistic Missile," *Journal of the Aero/Space Sciences*, Feb. 1958, pp. 94-98.

[6] Lichtenstein, J.H., "Analytical Investigation of the Dynamic Behavior of a Nonlifting Manned Re-Entry Vehicle," NASA TN D-416, Sept. 1960.

[7] Tobak, M., "Analytical Study of the Tumbling Motions of Vehicles Entering Planetary Atomspheres," NASA TN D-1549, Oct. 1962.

Large Fracture Toughness Boron-Epoxy Composites

A.G. Atkins*
University of Michigan, Ann Arbor, Mich.

In conventional brittle fiber/brittle filament composites, when the interfacial bond between filament and matrix is strong, fracture is often caused by rapid matrix cracks which break through all filaments in their paths. The toughness of such composites is low because, in general, the critical transfer length associated with strong interfacial bonding is small, which limits various components of total toughness—the 'surfaces' component, Piggott-Fitz-Randolph stress redistribution and Cottrell-Kelly pull-out (see, for

Presented as Paper 75-773 at the AIAA/ASME/SAE 16th Structures, Structural Dynamics, and Materials Conference, Denver, Colorado, May 27-29, 1975; submitted June 17, 1975; revision received July 30, 1975. I am pleased to thank NASA for a grant (NGR 23.005.528) under which most of this work was carried out.

Index categories: Materials, Properties of; Structural Composite Materials (including Coatings).

*Associate Professor of Mechanical Engineering.

example, Ref. 1). The critical length is given by $l_{crit} = \sigma_f d/2\tau$, where σ_f is the filament strength, d the filament diameter, and τ the interfacial shear strength. A general increase of l_{crit} by lowering the filament-matrix shear bond will increase the toughness, but weak interfaces throughout the composite reduce the tensile strength quite significantly.

Recent work[2,3] has shown that "intermittent bonding" allows high toughness to be obtained in brittle filament/brittle matrix composites without significant loss of tensile strength. Filaments are arranged to have alternate bands of high and low shear stress (and low and high toughness) by interrupted coating along the filaments with appropriate substances. The strong regions ensure that the filament strength is picked up; randomly positioned weak areas effectively blunt cracks by the Cook-Gordon mechanism[4] which in turn produces long pull-out lengths with an associated large contribution to toughness. Unidirectional boron-epoxy composites of volume fraction 0.20-0.25 have been made in this way; they have fracture toughnesses of over 200 kJ/m^2, (as opposed to about 40 kJ/m^2 with no coating), and they retain rule of mixtures tensile strengths (~650 MN/m^2). At the volume fractions used, that apparently represents K_{IC} values greater than 100 MN/m$^{-3/2}$, where K_{IC} is the critical stress intensity factor.

Two different coating materials have been investigated[2,3], viz: silicone vacuum grease (SVG) and polyurethane varnish (PUV). Both appear to produce similar interfacial shear strengths in the coated regions, since the tensile strength variations with coating geometry are indistinguishable. Their effects on toughness, however, are significantly different: SVG produces only a modest increase in toughness (up to say 60 kJ/m^2 as opposed to some 40 kJ/m^2 when uncoated), whereas PUV coatings give the previously quoted values of over 200 kJ/m^2. The difference is explained in terms of the occurrence of Cook-Gordon debonding with PUV, but its absence in SVG systems. Thus it seems that *interfacial toughness*, rather than the commonly considered *interfacial shear strength*, may be an important parameter controlling overall composite toughness. The relationships between interfacial toughnesses, in various debonding modes, and interfacial strengths are not clear.

This present paper reports the results of recent experiments with angle-ply layups rather than unidirectional composites. The absolute values of strength and toughness are of course lower, but in general terms the same trends are observed, with markedly improved toughness at high percentage PUV coatings.

Tensile strength and toughness specimens were made from layers of intermittently bonded, epoxy composite tape, manufactured on a drum apparatus with a device for coating the filaments, before layup,[3] with various coating/uncoating sequences. The tape (similar to Avco Rigidite, Prepreg tape) consisted of a 250 μm monolayer of B/W filaments in EPON 828 epoxy, backed, for ease of handling, on 760 mm wide nylon scrim cloth about 50 μm thick. Tensile specimens consisted of 5 layers of tape, arranged in the following orientation sequence $0°/+45°/0/-45°/0$, where 0° is the pulling direction. The specimens had a gauge section of some 60 mm x 6 mm x 1 mm. The toughness specimens were 7 layer flat coupon specimens (about 76 mm x 76 mm) with long starter cracks, akin to ASTM compact tension specimens[5] in profile. To prevent the composite arms above the crack from shearing off under load, an additional layer of tape was added to each side of the specimen, with filaments parallel to the crack. The central cores of the specimens thus consisted of 5 oriented filament layers in the path of the crack, where, within the limitations of the specimen and tape preparation method, the coated and uncoated layers occurred randomly relative to each filament. The starter crack in these edge crack specimens was made with a profiled diamond slitting wheel. Toughness was measured for increments of crack area, using Gurney's segmental area technique.[6]

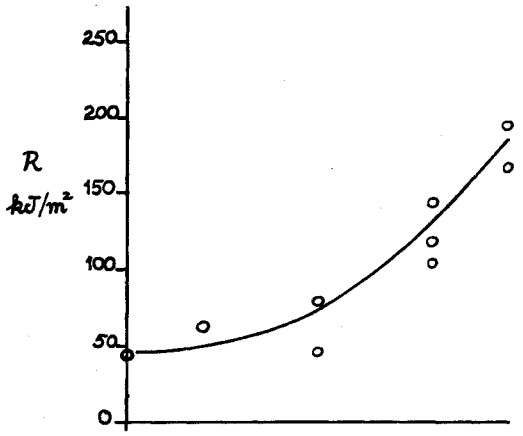

Fig. 1 Fracture toughness of 0.2 volume fraction boron/epoxy "compact tension" profile testpieces vs polyurethane varnish coated fraction.

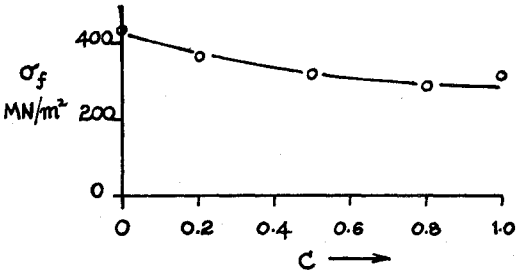

Fig. 2 Tensile strength of 0.2 volume fraction boron/epoxy specimens vs polyurethane varnish coated fraction.

Tensile strength and fracture toughness for the PUV coated crossply specimens are plotted in Fig. 1 and 2 against C, the coated fraction. $C = \ell_c/(\ell_c + \ell_{uc})$ where ℓ_c is the coated length, ℓ_{uc} the uncoated length and $(\ell_{c+\ell_{uc}})$ the repeat distance of the coating pattern along the filaments.

The promising results obtained earlier for unidirectional filaments have been duplicated in angle-ply layups. The absolute values of strength and toughness are less, of course, for the same volume fraction of filaments. Even so, quite respectable strengths and toughnesses are still obtained (300~400 MN/m^2 and 100~200 kJ/m^2 at the higher percentage coatings) coupled with less anisotropy. There is some scatter in the results (cf. the fracture toughness at $C=0.25$), but the trend is undoubtedly towards greater toughnesses at high coated fractions.

A significant contributor to total toughness is the pull-out work performed by those filaments bridging the crack face after passage of the main crack front. Such filaments, broken at distances removed from the main crack plane, can stabilize cracking in specimens that have bad geometric stability factors[7] and which would normally be unstable (e.g. the single edge notch (SEN) tensile specimen). Testpieces with filaments bridging the crack faces will not return to the origin upon unloading because of geometric interference (i.e. the filaments would have to be pushed back up the holes down which they had been pulled). Usually, when unloading lines do not go back to the origin, it is an indication of generalized yielding at regions remote from the crack tip (cf. the difficulties of testing metals, such as low carbon steels, which have large toughness-to-yield-strength ratios). A means of establishing whether gross irreversibilities have occurred away from the crack tip is to saw through the crack tip zone into virgin material beyond. If the crack then closes up, it may be assumed that the cause of remaining open was simply geometric interference on the part of the filaments, akin to a residual elastic opening moment at the crack tip. Such an investigation of displacement reversibility is important, since all fracture mechanics is predicated on this fact.

References

[1]Marston, T.U., Atkins, A.G., and Felbeck, D.K., "Interfacial Fracture Energy and the Toughness of Composites," *Journal of Materials Science*, Vol. 9, 1974, pp. 447-455.

[2]Atkins, A.G., Letter to *'Nature,'* Vol. 252, Nov. 1974, pp. 116-118.

[3]Atkins, A.G., "Intermittent Bonding for High Toughness/High Strength Composites," *Journal of Materials Science*, Vol. 10, 1975, pp. 819-832.

[4]Cook, J. and Gordon, J.E., "A Mechanism for the Control of Crack Propagation in All-Brittle Systems," Proceedings of the Royal Society (London) Vol. A282, 1964, pp. 508-520.

[5]ASTM, Special Technical Publication No. 463, 1970.

[6]Gurney, C. and Hunt, J., "Quasi-static Crack Propagation", Proceedings Royal Society, (London), Vol. A299, 1967, pp. 508-523.

[7]Gurney, C. and Mai, Y.W., "Stability of Cracking," *Engineering Fracture Mechanics*, Vol. 4, 1972, pp. 853-863.

Errata

Some Aspects of Fan Noise Suppression Using High Mach Number Inlets

S.D. Savkar
General Electric Company, Schenectady, N.Y.
and
S.B. Kazin
General Electric Company, Evendale, Ohio

[J. Aircraft **12**, 487-493) (1975)]

CORRECTED captions to Figs. 2, 8, 9, 10, 11, 12, 14 should read:

Fig. 2 Evolution of a rotor (cascade) MPT pattern using the nonlinear model of Kurosaka.[6] $B=53$ blades. $M_\infty=1.135$. Blade to blade spacing, $S=1.09$ in. Incidence for nominal stagger = 1.05°. Nominal stagger 65°. x = axial distance; ○ = uniform rotor; ◇ = 25th shaft harmonic; △ = 13th shaft harmonic; □ = BPF; ⬡ = 41st shaft harmonic.

Received September 9, 1975.
Index categories: Aircraft Noise, Aerodynamics (including Sonic Boom); Aircraft Aerodynamics (including Component Aerodynamics); Subsonic and Transonic Flow.

Fig. 8 Aerodynamic behavior of accelerating inlets—total pressure recovery correlated with one-dimensional geometric throat Mach number. ⌂ -inlet 1 (baseline); ◊ -inlet 2; ○ -inlet 3; ◇ -inlet 4. All inlets $L/d=1$. Inlet 4 has an extended high Mach number region and the shortest diffuser.

Fig. 9 Measured radiated sound power vs wheel speed for the GE-Corporate Research & Development tests. ⌂ -inlet 1 (baseline); ◊ -inlet 2; ○ -inlet 3; ◇ -inlet 4. Note the breaks in curves for inlets 2 and 3 which appear to be traceable to effects of unsteady shock boundary-layer interaction in the inlet throat.

Fig. 10 Noise reduction for the GE-Corporate Research & Development tests. Peak 200 ft sideline PNL tested for correlation with peak wall Mach number. All data referenced to inlet 1. -inlet 2; -inlet 3; -inlet 4.

Fig. 11 Noise reduction for the GE-Corporate Research & Development tests in terms of peak 200 ft sideline PNL. Correlation with respect to one-dimensional geometric throat Mach number. All data referenced to inlet 1. ◊ -inlet 2; ○ -inlet 3; ◇ -inlet 4.

Fig. 12 Noise reduction data for the GE-Corporate Research & Development tests (high-speed fan) in terms of radiated sound power level. -inlet 2; ○ -inlet 3; ◇ -inlet 4. - - - calculations using inlet 3 Mach number distribution. All data referenced to inlet 1.

Fig. 14 Composite of accelerating inlet noise reduction data—influence of wheel tip speed. ○ -½ scale fan data; ◇ -Langley high tip speed; △ -Langley low tip speed; ⬡ -GE-Corporate Research & Development tests (high-speed fan).